AD/RHIC–72


**R H I C  P R O J E C T**

Brookhaven National Laboratory
Associated Universities, Inc.
Upton, NY 11973


# Betatron Distortion Due to Linear Coupling and its Effects on the Dynamic Aperture in RHIC


G. Parzen



June 1990

# Betatron Distortion due to Linear Coupling and its Effects on the Dynamic Aperture in RHIC

G. Parzen

## 1. Introduction

The coupling introduced by the random $a_1$ can produce considerable distortion of the betatron motion. For a given initial $x_o$, $x'_o$, $y_o$, $y'_o$, maximum $x$ and the maximum $y$ for the subsequent motion can be considerably larger when coupling is present. The maximum $x$ and $y$ can be used as a measure of the betatron distortion.

One effect of this betatron distortion shows up in the dynamic aperture, in a loss in the stability limit, $A_{SL}$, found by tracking. The betatron distortion causes the particle to move further out in the magnets, where it sees stronger non–linear fields. The betatron distortion effect also shows up in a loss of linear acceptance. In injection and extraction, the larger betatron motion caused by the coupling requires more aperture.

Previous tracking[1] showed a loss in $A_{SL}$ due to random $a_1$ and $b_1$. It was noticed then that the loss in $A_{SL}$ was associated with a betatron motion distortion which was primarily a linear effect. For a given initial $x$, $x'$, $y$, $y'$ the $x_{\max}$ and $y_{\max}$ in the high–$\beta$ magnets were considerably larger (about 30% larger) for those random $a_1$ distributions which produced the smaller $A_{SL}$.

The studies described below show that the stability limit, $A_{SL}$, depends on the starting location around the ring. This variation in $A_{SL}$ around the ring can be correlated with the variation in the betatron distortion for particles starting at different places around the ring. It is proposed that the average of the $A_{SL}$ found by starting at each of the QF, the focusing quadrupoles in the arcs, can be taken as a measure of the dynamic aperture. It was found that the average $A_{SL}$ is reduced by about 15% by the random $a_1$ multipoles expected in RHIC.

## 2. $\beta$–Functions of the Normal Modes

Edwards and Teng showed how to transform to a new set of coordinates $v$, $v'$, $u$, $u'$ which are uncoupled.[2] These new normal coordinates are related to $x$, $x'$, $y$, $y'$ by a $4 \times 4$ matrix $R$

$$x = R \ v \ .$$

[1] G. Parzen, AD/RHIC–AP–80, 1989.

[2] D. Edwards and L. Teng, IEEE 1973 PAC, p. 885.

The normal coordinates have emittances $\epsilon_1$ and $\epsilon_2$ and $\beta$–functions $\beta_1$ and $\beta_2$. $\epsilon_1$ and $\epsilon_2$ are invariants. The $x$ and $y$ motion can be written as the sum of these two normal modes.

$\beta_1$ and $\beta_2$ and the $R$ matrix can be computed from the one turn transfer matrix. For RHIC, $\beta_1$ and $\beta_2$ can be considerably larger than $\beta_x$, $\beta_y$ by as much as 100% in the worse case found. However, the $x_{\max}$, $y_{\max}$ for a given initial $x$, $x'$, $y$, $y'$ are not simply related to $\beta_1$, $\beta_2$. To investigate $x_{\max}$, $y_{\max}$, the CDF, the coupling distortion function was introduced.

## 3. The Coupling Distortion Function

The coupling distortion function, CDF, describes $x_{\max}$, $y_{\max}$ for a given initial $x$, $x'$, $y$, $y'$. The CDF at the point $s$ is defined by

$$CDF = \frac{x_{\max}(s)}{x_{\max,\mathrm{nc}}(s)} \tag{3.1}$$

for a given initial $x$, $x'$, $y$, $y'$ at $s = s_o$. $x_{\max,\mathrm{nc}}$ is the $x_{\max}$ in the absence of coupling. For examining the loss in $A_{SL}$, $\epsilon_x = \epsilon_y$, $x' = y' = 0$ at the start is chosen. A corresponding CDF is defined for the $y$ motion.

To compute CDF, one has to compute $x_{\max}(s)$ in the presence of coupling. An analytical result was found for $x_{\max}(s)$ in terms of $\beta_1$, $\beta_2$, $\epsilon_1$, $\epsilon_2$ and the $R$ matrix. This result is given in Section 6.

Table 1 lists the coupling distortion function, CDF, and the $\beta$–functions of the normal modes, $\beta_1$ and $\beta_2$ for ten different distributions of the random field errors. The random quadrupole errors are described in section 7. The CDF is the largest CDF found at any of the high $\beta$ quadrupoles in the insertions for either $x$ or $y$ motion for a particle starting at the focusing quadrupole in the middle of the first arc in RHIC. The $\beta_1$, $\beta_2$ are the largest $\beta$–functions of the normal modes found around the accelerator. For $a_1 = b_1 = 0$, the largest $\beta$ functions are $\beta = 220$ m for $\beta^* = 6$ and $\beta^* = 630$ for $\beta^* = 2$. A CDF as large as CDF $= 2.1$ is found for one field error distribution. A simple picture of coupling would suggest CDF $\simeq 1.4$ resulting from a complete exchange of the emittance between the $x$ and $y$ motions. The betatron distortion is about 40% larger for the worst case than what one would expect from the simple picture of a complete exchange of the emittances.

Table 1. CDF at High $\beta$ Quads

| Field Error Number | $\beta^* = 6$ | | | $\beta^* = 2$ | | |
|---|---|---|---|---|---|---|
| | CDF | $\beta_1$(m) | $\beta_2$(m) | CDF | $\beta_1$(m) | $\beta_2$(m) |
| 1 | 1.47 | 246 | 236 | 1.32 | 695 | 684 |
| 2 | 1.38 | 266 | 264 | 1.46 | 650 | 644 |
| 3 | 1.29 | 237 | 244 | 1.30 | 682 | 744 |
| 4 | 1.52 | 254 | 249 | 1.55 | 723 | 797 |
| 5 | 1.48 | 255 | 260 | 1.10 | 766 | 752 |
| 6 | 1.43 | 230 | 223 | 1.38 | 625 | 654 |
| 7 | 1.67 | 250 | 224 | 2.10 | 956 | 970 |
| 8 | 1.71 | 305 | 284 | 1.63 | 816 | 764 |
| 9 | 1.33 | 237 | 243 | 1.30 | 687 | 655 |
| 10 | 1.33 | 255 | 248 | 1.35 | 797 | 670 |

There is some correlation between CDF and $\beta_1$ and $\beta_2$. However, the CDF depends not only on $\beta_1$, $\beta_2$ but also on the mismatch in the emittances. For the given initial $\epsilon_x$, $\epsilon_y$, the corresponding $\epsilon_1$, $\epsilon_2$ may be larger than $\epsilon_x$, $\epsilon_y$.

Table 2 shows the correlation between the CDF and the dynamic aperture which is measured by $A_{SL}$. $A_{SL}$ is found from tracking studies with the random field errors, including higher multipoles, present. $A_{SL}$ is the largest stable initial $x$ with the starting conditions $\epsilon_x = \epsilon_y$, $x' = y' = 0$, and starting at the focusing quadrupole at the middle of the first arc in RHIC.

The correlation between the coupling distortion function, CDF, and the dynamic aperture $A_{SL}$ is good. Note that the $A_{SL}$ are computed after the coupling has been corrected[3] using the $a_1$ correctors at Q2 and Q5.

Table 2. Correlation of the CDF and $A_{SL}$

| Field Error Number | $\beta^* = 6$ | | $\beta^* = 2$ | |
|---|---|---|---|---|
| | CDF | $A_{SL}$ (mm) | CDF | $A_{SL}$ (mm) |
| 1 | 1.47 | 14.5 | 1.32 | 8.5 |
| 2 | 1.38 | 14.5 | 1.46 | 6.5 |
| 3 | 1.29 | 15.5 | 1.30 | 8.5 |
| 4 | 1.52 | 15.5 | 1.55 | 7.5 |
| 5 | 1.48 | 14.5 | 1.10 | 8.5 |
| 6 | 1.43 | 16.5 | 1.38 | 8.5 |
| 7 | 1.67 | 12.5 | 2.10 | 4.5 |
| 8 | 1.71 | 12.5 | 1.63 | 6.5 |
| 9 | 1.33 | 16.5 | 1.30 | 8.5 |
| 10 | 1.33 | 14.5 | 1.35 | 7.5 |

[3] G. Parzen, AD/RHIC–AP–72 (1988).

In the absence of the random $a_1$, $b_1$, the stability limit has been found to be $A_{SL} = 15.5$ mm for $\beta^* = 6$ and $A_{SL} = 7.5$ mm for $\beta^* = 2$. The results in Table 2 indicate that for this particular starting place around the ring, $A_{SL}$ has been reduced to $A_{SL} = 4.5$ mm for $\beta^* = 2$ m. The dependence of $A_{SL}$ on the starting location around the ring is discussed in section 4.

The large CDF, CDF $\sim 2$ found above can be correlated with the nearby sum resonances $\nu_x + \nu_y = 58$ and $\nu_x + \nu_y = 57$. This is useful in finding a correction system to reduce the large CDF.

## 4. Azimuthal Dependence of CDF and $A_{SL}$

In the previous tables, CDF and $A_{SL}$ were computed at the middle QF in the first inner arc in RHIC. If one computes CDF starting at different QF, CDF will change and thus $A_{SL}$ will also change. $\beta_1$ and $\beta_2$ will also change.

If the particle is started at different QF, the value of CDF, $A_{SL}$ and $\beta_1$, $\beta_2$ will change at each QF. Figure 1 shows this variation in CDF and $\beta_1$ at the 12 QF in the first arc. Roughly, CDF and $\beta_1$ oscillate around the ring. The CDF plotted is the largest CDF found at the high–$\beta$ quadrupoles in the insertions, when the particle is started at different QF.

It is likely that $A_{SL}$ will also oscillate around the ring, since $A_{SL}$ and CDF are well correlated. In Fig. 2 $A_{SL}$ is plotted versus CDF for a particle starting at 5 different QF in the ring. These 5 points include the largest and smallest CDF found in the ring. $A_{SL}$ is computed at the QF at which the particle is started.

Since $A_{SL}$ now depends on which QF the particle is started at, one has the problem of which value of $A_{SL}$ is to be used for the dynamic aperture. The procedure used here is to find the average $A_{SL}$ using the $A_{SL}$ found at all the QF in the ring.

To compute $A_{SL,av}$ the average $A_{SL}$, one should in principle compute $A_{SL}$ at all the QF in the ring and then compute the average $A_{SL}$. This would require a good deal of effort. Instead, the following procedure was used. The coupling distortion function at the high $\beta$ quadrupole is computed starting at each QF in the ring. One then locates the QF that give the largest and smallest CDF, $\mathrm{CDF_{max}}$ and $\mathrm{CDF_{min}}$. The stability limit $A_{SL}$ is computed starting at these two QF. It is assumed that this gives the largest and smallest $A_{SL}$, $A_{SL,max}$ and $A_{SL,min}$. The average $A_{SL}$ is then computed as

$$A_{SL,av} = \frac{1}{2}(A_{SL,max} + A_{SL,min})$$

The computation of $A_{SL,av}$ for the two worst field errors, errors 7 and 8, are shown in Table 3.

Table 3. Computation of $A_{SL,av}$

| $\beta^*$ | Error No. | $A_{SL,max}$ | $A_{SL,min}$ | $A_{SL,av}$ | CDF Max | CDF Min |
|---|---|---|---|---|---|---|
| 6 | 7 | 14.5 | 11.5 | 13 | 1.67 | 1.29 |
| 6 | 8 | 16.5 | 10.5 | 13.5 | 2.0 | 1.24 |
| 2 | 7 | 8.5 | 4.5 | 6.5 | 2.1 | 1.10 |
| 2 | 8 | 8.5 | 6.5 | 7 | 1.8 | 1.21 |

The loss in $A_{SL}$ is now 15%. $A_{SL}$ has been decreased from 15.5 mm to 13 mm, for $\beta^* = 6$ from 7.5 mm to 6.5 mm for $\beta^* = 2$.

Figure 3 shows the maximum and minimum CDF found by starting at each QF in the ring for the ten different error distributions. The dashed line at CDF = 1.414 is the value of CDF expected using the simple picture of a complete exchange of $\epsilon_x$ and $\epsilon_y$ between the $x$ and $y$ motions. This plot shows that error distributions that do not show much loss in $A_{SL}$ still may have a CDF appreciably larger than CDF = 1.414.

## 5. Loss in Linear Acceptance

The loss in linear acceptance due to the betatron distortion may be more serious than the loss in dynamic aperture. For injection the injected beam could be much larger because of the betatron distortion. For extraction, the extraction magnet could be off by quite a bit in its location in order to accept the required emittance of $6\pi$. The correction of the betatron distortion (the CDF) appears important.

It may be possible to design an $a_1$ correction system that corrects the betatron distortion all around the ring. The system of separately excited $a_1$ near each Q2, previously proposed,[4] may correct this betatron distortion to a certain extent.

## 6. Analytical Results for $X_{\max}$ and $Y_{\max}$

In this section, analytical results are given for the maximum $x$ and $y$, $x_{\max}$ and $y_{\max}$, that will be reached for a particle with a given initial $x$, $x'$, $y$, $y'$ in the presence of coupling. These results are needed in order to compute the coupling distortion function, CDF. Derivations of these results will be given in a future paper.

[4] G. Parzen, AD/RHIC/AP–89, 1990.

For a given set of initial $x$, $x'$, $y$, $y'$, $x_{\max}$ and $y_{\max}$ are given by

$$\begin{aligned} x_{\max} &= (\beta_1\epsilon_1)^{\frac{1}{2}}\cos\phi + (\beta_{x,2}\epsilon_2)^{\frac{1}{2}}\sin\phi, \\ \beta_{x,2} &= \bar{D}_{11}^2\beta_2 + \bar{D}_{12}^2\gamma_2 + 2\bar{D}_{11}\bar{D}_{12}\alpha_2, \\ y_{\max} &= (\beta_2\epsilon_2)^{\frac{1}{2}}\cos\phi + (\beta_{y,1}\epsilon_1)^{\frac{1}{2}}\sin\phi, \\ \beta_{y,1} &= D_{11}^2\beta_1 + D_{12}^2\gamma_1 + 2D_{11}D_{12}\alpha_1 \ . \end{aligned} \tag{6.1}$$

$D$ and $\bar{D}$ are $2\times 2$ matrices, which together with $\phi$ define the $4\times 4$ $R$ matrix, defined in section 2. $R$ is given by

$$R = \begin{pmatrix} I\ \cos\phi & D\ \sin\phi \\ -\bar{D}\ \sin\phi & I\ \cos\phi \end{pmatrix} \tag{6.2}$$

$\bar{D} = D^{-1}$, $|D| = 1$ and $I$ is the $2\times 2$ identity matrix.

$\beta_1$, $\alpha_1$, $\gamma_1$ and $\beta_2$, $\alpha_2$, $\gamma_2$ are the orbit parameters of the normal modes, $\epsilon_1$ and $\epsilon_2$ are the emittances of the normal odes that correspond to the initial $x$, $x'$, $y$, $y'$.

One can also find expressions for $x'_{\max}$ and $y'_{\max}$. These are given by

$$\begin{aligned} x'_{\max} &= (\gamma_1\epsilon_1)^{\frac{1}{2}}\cos\varphi + (\gamma_{x,2}\epsilon_2)^{\frac{1}{2}}\sin\phi, \\ \gamma_{x,2} &= \bar{D}_{21}^2\beta_2 + \bar{D}_{22}^2\gamma_2 + 2\bar{D}_{21}\bar{D}_{22}\alpha_2, \\ y'_{\max} &= (\gamma_2\epsilon_2)^{\frac{1}{2}}\cos\varphi + (\gamma_{y,1}\epsilon_1)^{\frac{1}{2}}\sin\phi, \\ \gamma_{y,1} &= D_{21}^2\beta_1 + D_{22}^2\gamma_1 + 2D_{21}D_{11}\alpha_1 \ . \end{aligned} \tag{6.3}$$

Edwards and Teng[2] describe how to compute the $R$ matrix and $\beta_1$, $\alpha_1$, $\gamma_1$ and $\beta_2$, $\alpha_2$, $\gamma_2$ from the one turn transfer matrix. This then allows one to compute $\epsilon_1$ and $\epsilon_2$ from the initial $x$, $x'$, $y$, $y'$. Equation 6.1 can then be used to compute $x_{\max}$ and $y_{\max}$ for the given initial $x$, $x'$, $y$, $y'$, which is needed to compute the coupling distortion function, CDF (see Eq. (3.1) for CDF).

## 7. Random $a_1$, $b_1$ Present in RHIC

The random quadrupole errors are due to a number of sources that include construction errors in the magnet coils, effective length errors in the quadrupoles, and rotational errors in the positioning of the quadrupoles.

$a_1$ and $b_1$ are defined so that the field due to $a_1$ and $b_1$ on the median plane is given by

$$\begin{aligned} B_y &= B_0 b_1 x \\ B_x &= B_0 a_1 x \end{aligned}$$

where $B_0$ is the main dipole field.

The rms random $a_1$, $b_1$ used in this study are given in the following table.

| Source | $a_1/10^{-5}$ ($\mathrm{cm}^{-1}$) | $b_1/10^{-5}$ ($\mathrm{cm}^{-1}$) |
|---|---|---|
| Dipole coil error | 16.8 | 8.4 |
| Quadrupole coil error | 15 | 15 |
| Quadrupole effective length | — | 40 |
| Quadrupole rotation error | 40 | — |

The assumed effective length error in the quadrupoles is $\Delta L/L = 2 \times 10^{-3}$ rms. The assumed rotational error in the quadrupoles is $\Delta\theta = 1 \times 10^{-3}$ rad rms.

Fig. 1. $\beta_1$ and CDF at different $Q_F$

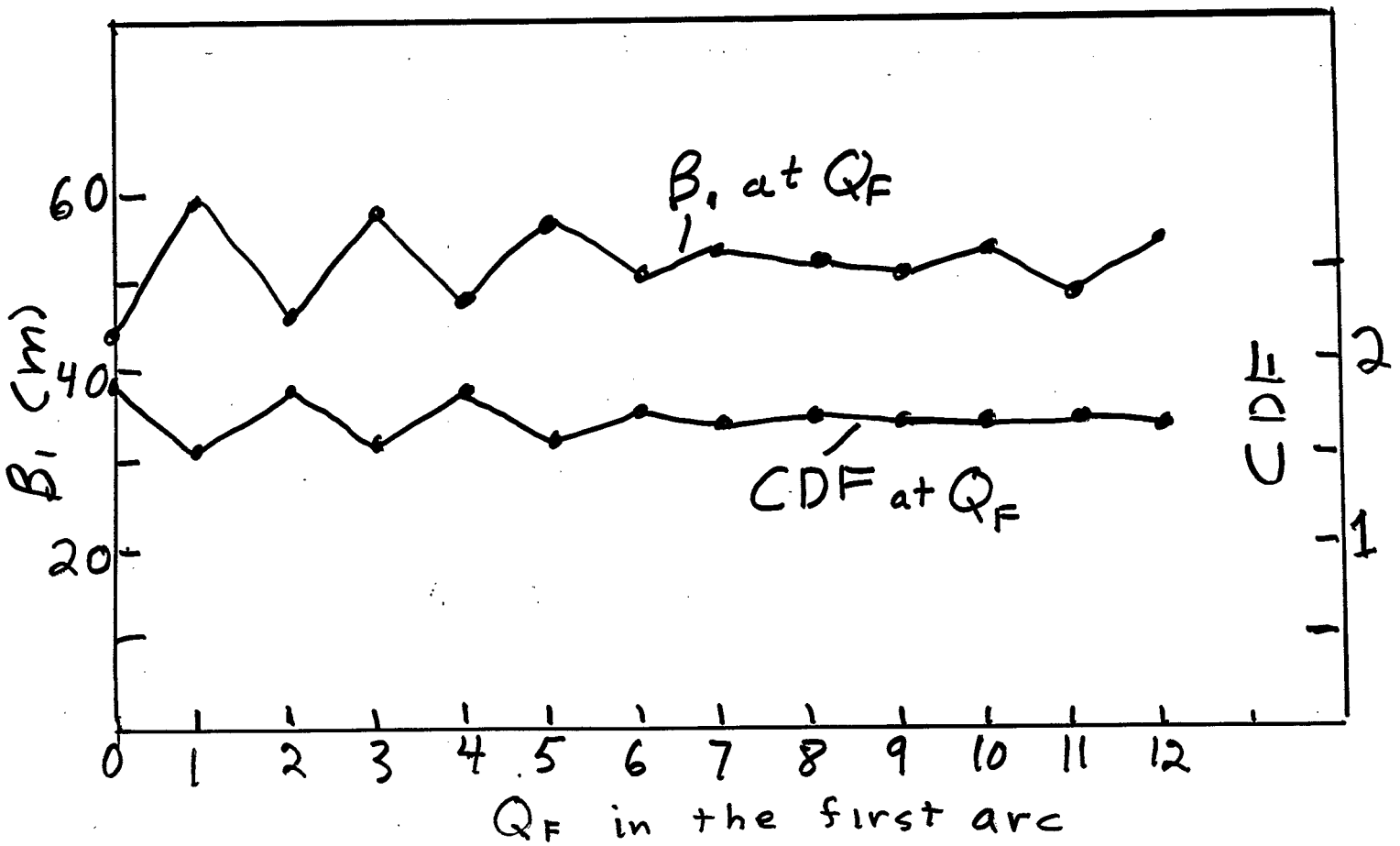

Fig. 2. Stability Limit, $A_{SL}$, versus CDF

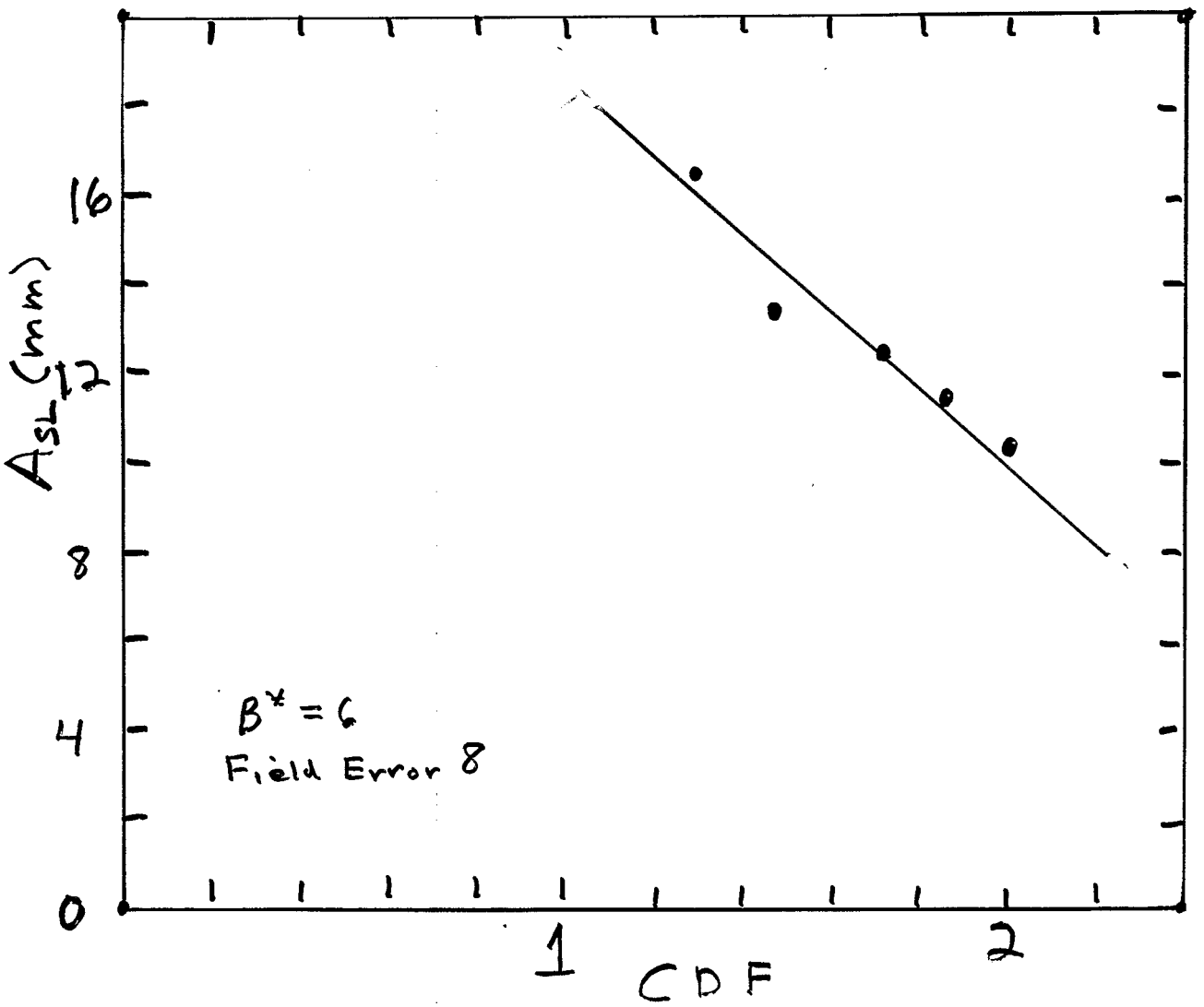
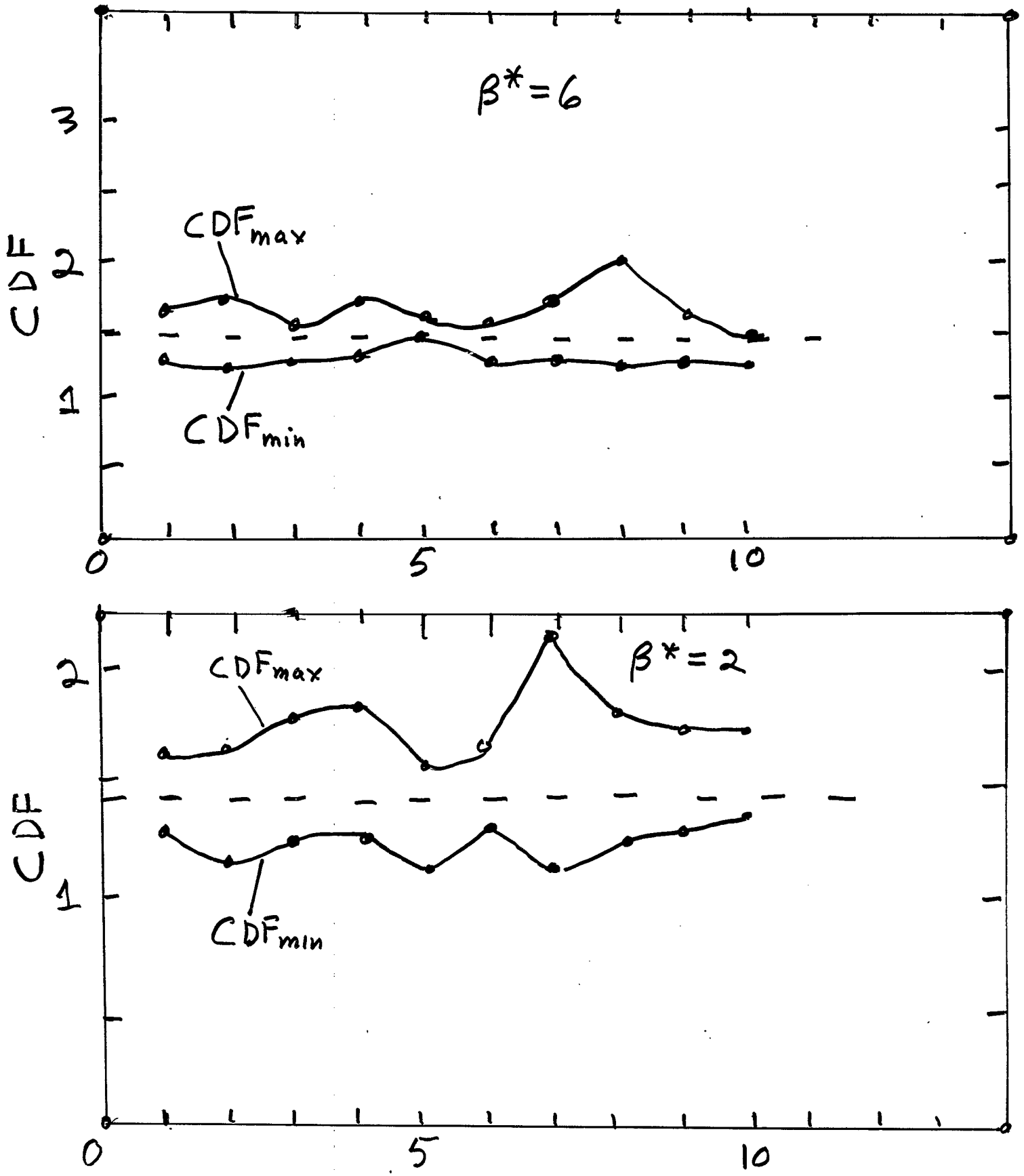
Fig 3. CDF for 10 Random Field Errors